CrossMark

P2X7 Receptors Mediate CO-Induced Alterations in Gene Expression in Cultured Cortical Astrocytes—Transcriptomic Study

Sara R. Oliveira [1,2,3] · Cláudia Figueiredo-Pereira [2] · Carlos B. Duarte [1,4] · Helena L. A. Vieira [2,5]

Abstract

Carbon monoxide (CO) is an endogenous gasotransmitter that limits inflammation and prevents apoptosis in several tissues, including the brain. Low concentrations of CO are cytoprotective in astrocytes, neurons, and microglia, but the underlying molecular mechanisms remain poorly understood. This work aims at identification of alterations in gene expression conferred by CO in primary cultures of cortical astrocytes, for further disclosure of the molecular mechanism of action of the gasotransmitter. Astrocytes were treated with the CO-releasing molecule CORM-A1 for 40 min, and transcriptional changes were analyzed using RNASeq. A total of 162 genes were differentially expressed in response to CO treatment, and 7 of these genes were selected for further analysis: FosB, Scand1, Rgs10, Actg1, Panx1, Pcbdh21, and Rn18s. The alterations in their expression were further validated using qRT-PCR. An increase in FosB protein expression was also observed after 40 min of CORM-A1 treatment, as determined by a western blot. CO-induced FosB expression and cytoprotection were both abrogated in the presence of the P2X7 receptor antagonist A-438079. Furthermore, CORM-A1 increased phosphorylation of calcium/calmodulin-dependent protein kinase II (CaMKII), which is a downstream event of P2X7R activation. The functional importance of FosB in CO-induced survival was assessed by knocking down its expression with FosB siRNA. Astrocytes were challenged to death with oxidative stress and cell viability was assessed 24 h later. Downregulation of FosB did not prevent the effects of CO in the inhibition of astrocytic cell death. Nevertheless, the transcriptomic changes observed upon treatment of astrocytes with CO open new opportunities for further studies on CO cytoprotective pathways.

Keywords Carbon monoxide · Astrocytes · FosB · Cytoprotection · P2X7R · Transcriptome

✉ Helena L. A. Vieira
helena.vieira@nms.unl.pt

1 CNC- Center for Neuroscience and Cell Biology, University of Coimbra, Coimbra, Portugal

2 CEDOC, Chronic Diseases Research Centre, NOVA Medical School/Faculdade de Ciência Médicas, Universidade Nova de Lisboa, 1169-056 Lisbon, Portugal

3 Institute for Interdisciplinary Research (IIIUC), University of Coimbra, Coimbra, Portugal

4 Department of Life Sciences, University of Coimbra, Coimbra, Portugal

5 Instituto de Biologia Experimental e Tecnológica (iBET), Apartado 12, 2781-901 Oeiras, Portugal

Abbreviations

Actg1	Actin gamma 1
AP-1	Activator protein 1
ATF	Activating transcription factor
Bcl-2	B cell leukemia/lymphoma 2
BDNF	Brain-derived neurotrophic factor
CBP	CREB binding protein
CaMKII	Ca^{2+}/calmodulin-dependent protein kinase II
CO	Carbon monoxide
CORM-A1	Carbon monoxide-releasing molecule A1
CREB	cAMP-response element-binding protein
DEGs	Differentially expressed genes
ERK	Extracellular signal-regulated kinase
FRK	Fos-regulating kinase
Gapdh	Glyceraldehyde-3-phosphate dehydrogenase
HO-1	Haem oxygenase-1
Hprt1	Hypoxanthine guanine phosphoribosyl transferase I

JAK	Janus kinase
JNK	c-Jun N-terminal kinase
MAPK	Mitogen-activated protein kinase
MMP	Mitochondria membrane potential
NAC	N-acetylcysteine
Ppia	Peptidylprolyl isomerase A
PPARγ	Peroxisome proliferator-activated receptor gamma
PI	Propidium iodide
P2X7R	P2X7 receptor
qRT-PCR	Quantitative real-time reverse transcription-polymerase chain reaction
Rn18s	18S rRNA
Sdha	Succinate dehydrogenase complex, subunit A
sGC	Soluble guanylyl cyclase
siRNA	Small interfering RNA
SRE	Serum response element
t-BHP	tert-Butyl hydroperoxide
TCF	Ternary complex factor
TRE	12-O-Tetradecanoylphorbol-13-acetate (TPA) response element (consensus sequence 5′-TGAG/CTCA-3′)

Introduction

Carbon monoxide (CO) is an endogenously produced gasotransmitter, generated by the activity of haem oxygenase (HO), which confers cytoprotection by boosting cellular resistance against a wide variety of harmful events [1]. In the CNS, low concentrations of exogenous CO and/or expression of haem oxygenase-1 (HO-1) promote neuroprotection by limiting neuroinflammation and neural cell death, as well as by modulating vasodilation (for review, see [2]). Thus, CO was shown to have anti-apoptotic properties in neurons [3, 4] and in astrocytes [5, 6], promotes neurogenesis [7], and reduces neuroinflammation by acting on microglia [8–11]. Likewise, administration of low doses of CO improved the outcome in several rodent models of brain diseases, namely, ischemic stroke [12, 13], hemorrhagic stroke [14], and multiple sclerosis [15, 16]. Although several cytoprotective properties have been described for CO, the molecular mechanisms underlying the effects of CO are far away from being totally understood. Up to date, no transcriptomic study following exogenous CO treatment has been performed to identify the alterations in gene expression that contribute to CO-induced cytoprotection.

Because CO holds great potential for therapeutic purposes, several strategies based on the use of small molecules to deliver CO gas under controlled conditions have been developed. These molecules were first called CO-releasing molecules (CORM) [17] and several issues must be overcome before they can be used in biological systems, namely, water insolubility, toxic chemical structures, promotion of high levels of carboxyhemoglobin and chemical instability, among others [18]. CORM-A1 presents as main advantages the fact that it is water soluble and a slow CO releaser under physiological conditions; in fact, CORM-A1 releases CO in a pH- and temperature-dependent manner [19].

Astrocytes are the most abundant cell type in the brain and provide structural, metabolic, and trophic support to other neural cells, in particular to neurons [20]. Because of the tightly regulated crosstalk between neurons and astrocytes, one can suggest that improving astrocytic function can promote neuroprotection. Astrocytes show a high activity of different signaling pathways such as p38/MAPK, ERK, and PPAR [21–23], which are modulated by low concentrations of CO [24, 25]. Also, astrocytes are metabolically very active cells, being key players in brain metabolism, in particular in astrocyte-neuron lactate shuttle [26]. Likewise, some of the biological effects of CO have been attributed to regulation of cell metabolism [6, 11, 27, 28]. Finally, CO-induced modulation of astrocytic metabolism increased neuronal survival in a co-culture system subjected to oxidative stress conditions [29]. However, the effects of CO on gene expression in astrocytes, and the downstream events responsible for the protection of the nervous system have not been elucidated.

The aims of this work were (i) to identify putative molecular effectors of CO-induced cytoprotection in astrocytes by mRNA sequencing, (ii) to validate a set of these differentially expressed genes (DEGs) at the mRNA and protein levels, and finally (iii) to functionally validate the gene that shows more robust changes in expression following stimulation of astrocytes with CO, FosB. In the latter set of experiments, we investigated the putative role of this immediate early gene in mediating CO-induced protection in astrocytes subjected to oxidative stress conditions. The characterization of CO-induced alterations in gene expression will contribute to a better understanding of the CO-induced cytoprotective pathways and to the potential development of novel therapeutic strategies against cerebral diseases.

Material and Methods

Cortical Astrocyte Cultures

Primary cultures of mouse cortical astrocytes were prepared from the cortices of P1–P2 Bl6/c57 mice pups after mechanical dissociation, as previously described [30]. Briefly, cerebral hemispheres were carefully freed of meninges and the dissected cortices were washed in ice-cold PBS, dissociated mechanically, and passed through a 70-µm nylon cell strainer (BD Falcon™) into Dulbecco's minimum essential medium containing 1 g/L glucose (D5523, Sigma) and supplemented with 20% (v/v) fetal bovine serum (FBS; Gibco® Life Technologies) and 1% (v/v) penicillin/streptomycin (15070-063, Gibco® Life Technologies). Single-cell suspensions

were plated in T-flasks (eight to ten cortices/75 cm^2, Orange Scientific) and maintained in a humidified atmosphere of 5% CO_2/95% air at 37 °C. After 8 days in culture, the phase dark cells growing on the astrocytic cell layer were detached by vigorous shaking and removed. Culture medium was replaced twice a week for 3 weeks with gradual reduction in FBS content (2nd week 15%; 3rd week 10%). The confluent astrocytic cultures were mildly trypsinized (0.05% *w/v* trypsin/EDTA, 25300-104, Gibco®) and subcultured in six-well plates until full confluence.

Administration of CO to Astrocytic Culture

CORM-A1, a CO releasing molecule [19], was used to deliver CO to astrocytes. CORM-A1 (Sigma) stock solutions were prepared in water to a final concentration of 10 mM and stored at − 20 °C to avoid loss of released CO. Immediately before the experiments, CORM-A1 was diluted in PBS buffer to the indicated final concentration. CO-depleted inactive form (iCORM-A1) was generated to be used as negative control by initially dissolving CORM-A1 in 0.1 M HCl and then bubbling pure N_2 through the solution for 10 min in order to remove the residual CO gas. The solution of iCORM-A1 was finally adjusted to pH 7.4. PBS was saturated by bubbling 100% of CO gas for 30 min to produce 1 mM stock solution. Time points for CORM-A1 treatment were selected based on the cytoprotective effects of CO in astrocytes subjected to oxidative stress (data not shown). RNA extraction for RNASeq experiments was performed after 40 min of incubation with CORM-A1 (12.5 μM); for qRT-PCR experiments, the cells were incubated with CORM-A1 for 30 min, 40 min, and 60 min at a final concentration of 12.5 μM. Protein extracts were prepared at 40 min, 1 h, 2 h, 3 h, 4 h, and 5 h, following CORM-A1 administration. Non-supplemented PBS was added to control experiments without CORM-A1 treatment.

Total RNA Isolation and Assessment of Quality and Concentration of RNA

For RNA sequencing, astrocytes were cultured at 75 cm^2 T-flasks for each condition (two control conditions and two CO-treated conditions) and used when total confluency was reached. RNA was purified using RNeasy Qiagen kit according to the manufacturer's protocol, followed by lyophilization. A total amount of 15 μg of dried RNA per sample was sent to BGI (Copenhagen, Denmark) for RNA sequencing using the Illumina 2000 HiSeq instrument.

For qRT-PCR experiments, the full content of a six-well cluster plate, with a density of $4.5 × 10^5$ cells/well, was collected for each experimental condition and total RNA from cortical astrocytes was extracted with TRIzol (Invitrogen Life Technologies), following the manufacturer's specifications. After addition of chloroform and phase separation, the RNA

was precipitated with isopropanol. The precipitated RNA was washed once with 75% ethanol, centrifuged, air dried, and resuspended in 20 μL of RNase-free water (Gibco Life Technologies). The whole procedure was performed at 4 °C. RNA concentration and purity were determined by spectrophotometry (NanoDrop 2000; Thermo Scientific). RNA quality and integrity were assessed using the Experion RNA StdSens automated gel electrophoresis system (Bio-Rad). A virtual gel was created for each sample, allowing the detection of degradation of the reference markers RNA18S and 28S. The system labels each sample with a RNA Quality Indicator (RQI), ranging from 1 to 10. Samples were discarded when showing RQI ≤ 7, indicating that they presented RNA degradation, poor integrity, or contamination by DNA. Samples were stored at − 80 °C until further use in qRT-PCR.

Reverse Transcription PCR

For cDNA synthesis, 1 μg of total RNA was reverse transcribed using iScript™ cDNA Synthesis Kit (Bio-Rad) according to manufacturer instructions. Briefly, the samples were thawed on ice, and the PCR reaction mix was added to a 20-μL final volume. The reaction protocol started with a 5-min step at 25 °C, followed by 30 min at 42 °C and ended with a 5-min step at 85 °C (T100™ Thermal Cycler, Bio-Rad). Samples were stored at − 20 °C until further use.

Primer Design

Primers for real-time PCR were designed by Beacon Designer 8.13 software (Premier Biosoft International) as described in previous work [31]. The primers used are described in detail in Table S1.

Real-time PCR

For the gene expression studies, 2 μL of 1:10 diluted cDNA was added to 10 μL 2× SsoFast™ EvaGreen Supermix (Bio-Rad), and the final concentration of each primer was 250 nM in 20 μL final volume. The thermocycling reaction was initiated with activation of Sso7d-fusion DNA polymerase by heating at 95 °C during 30 s, followed by 40 cycles of a 10-s denaturation step at 95 °C, a 30-s annealing step at 55 °C, and a 30-s elongation step at 72 °C. The fluorescence was measured after the extension step by the iQ™5 Multicolor Real-Time PCR Detection System (Bio-Rad). After the thermocycling reaction, the melting step was performed, from 55 up to 95 °C, with an increment of 0.5 °C each 10 s. Continuous measurement of fluorescence allowed the detection of possible nonspecific products. The assay included a non-template control and a standard curve (three 1:10 sequential dilution steps) of cDNA for assessing the efficiency of all

primer pairs. The reactions were run in duplicate to reduce confounding variance and average results were calculated.

Gene Expression Analysis

Since all primer pairs presented an efficiency close to 100%, the data were processed using the $2^{-\Delta Ct}$ method, an adapted version of the $2^{-\Delta\Delta Ct}$ method [32], with $\Delta C_t = C_{t \text{ condition x}} - C_{t \text{ control}}$. The control corresponds to the reference condition representing 1-fold expression of each gene. The threshold cycle (C_t) refers to the cycle at which the fluorescence signal is detectable above background due to the accumulation of amplified product. This value is proportional to the starting copy number of the target sequence. C_t was measured in the exponential phase and, therefore, it was not affected by possible limiting components in the reaction. All C_t values were normalized to two internal control genes, Gapdh and Ppia, which were already validated to be the most suitable ones for the conditions used in this study [31]. For every run performed, the threshold was set at the same fluorescence value (100 RFU).

Total Protein Isolation and Concentration Calculation

After washing the astrocytes twice with ice-cold PBS (137 mM NaCl, 2.7 mM KCl, 1.8 mM K_2HPO_4, 10 mM $NaH_2PO_4\cdot2H_2O$), total protein was extracted using RIPA lysis buffer (150 mM NaCl, 50 mM Tris-HCl, 5 mM EGTA, 1% Triton X-100, 0.5% Deoxycholic acid, 0.1% Sodium dodecyl sulfate) freshly supplemented with 1X cocktail protease inhibitor (Roche, #11697498001, pH 7.5). The cells were then scraped and samples were stored at -20 °C until further use. Protein concentration was quantified using a bicinchoninic acid (BCA) protein assay kit (#23227, Pierce®) using the manufacturers' specifications. Absorbance was measured using a TECAN infinite F200PRO microplate reader.

Immunoblotting

Samples from cell extracts were separated under reducing electrophoresis on a 1-mm thick 12% sodium dodecyl sulfate-polyacrylamide (SDS-PAGE) gel. Samples were transferred to a nitrocellulose membrane (HybondTMC extra, GE Healthcare). FosB and the Ca^{2+}- and calmodulin-dependent protein kinase II (CaMKII) were stained with specific antibodies overnight at 4 °C (anti-FosB antibody: Santa Cruz Biotechnology, 1:333 dilution; anti-CaMKII antibody: Invitrogen MA1-047, 1:1000 dilution; anti phosphor-CaMKII: Santa Cruz Biotechnology sc-9035, 1:200 dilution). Blots were developed using the ECL (enhanced chemiluminescence) detection system after incubation with HRP-labeled anti-rabbit IgG antibody (1:5000 dilution) (GE Healthcare), for 1 h at room temperature.

siRNA Transfection

FosB expression was silenced by FosB coding siRNA transfection according to the manufacturer's instructions (Invitrogen). Astrocytes at 40% of confluence were transfected using Lipofectamine^{TM} RNAiMAX and OptiMEM® medium (Invitrogen); for 2 cm^2 of astrocytic culture area, 6 pmol of siRNA were used. siRNA and culture medium were mixed gently with Lipofectamine at room temperature, to form liposomes, and the astrocytes were then transfected in the absence of antibiotics.

Viability Analysis by Flow Cytometry

To detect apoptosis induced by *tert*-butyl hydroperoxide (t-BHP), the cells were collected by trypsinization, and stained with propidium iodide (1 g/ml) (Invitrogen) to determine cell viability, based on plasma membrane integrity. A flow cytometer (Canto II) was used to analyze apoptosis-associated parameters. This cytometer contains a blue solid state laser (488 nm) with FL3 red fluorescence channel for propidium iodide detection at 650 nm. The acquisition was done with Diva software and data analysis was performed with Flowing software (http://www.uskonaskel.fi/flowingsoftware/).

Administration of Chemical Compounds to Astrocytic Cultures

The stock solution of A-438079 (Sigma), a specific P2X7 receptor inhibitor [33, 34], was prepared in PBS to a final concentration of 2.5 mM and stored at -20 °C. Astrocytic cultures were incubated with 10 μM of A-438079. Non-supplemented PBS was added to control experiments.

Statistical Analysis

Data are presented as the mean ± standard error of the mean (SEM). The Student *t* test, and the one-way or two-way analysis of variance (ANOVA) tests were used in statistical analysis. ANOVAs were followed by the Dunnett or the Tukey multiple comparison tests. Statistical analysis was performed using GraphPad Prism 6 (GraphPad Software, Inc.).

Results

CO-Induced Differential Gene Expression in Cortical Astrocytes

In previous studies, we showed that CO prevents astrocytic cell death [5, 6]. Accordingly, pre-treatment of primary cultures of astrocytes with CORM-A1 for 1 h prior to stimulation with the pro-oxidant t-BHP reduced cell death assessed with

propidium iodide, which evaluates plasma membrane permeability (Fig. 1). Optimal concentration of CORM-A1 was chosen as descried in Supplementary Figure S1.

To investigate the molecular mechanisms underlying the protective effects of CO in astrocytes, we performed a transcriptional profiling via RNASeq. Primary cultures of mice cortical astrocytes were stimulated with 12.5 μM CORM-A1 ($t_{1/2} = 21$ min at 37 °C and pH = 7.4). Alterations in gene expression due to CO exposure were previously described to occur within 30 to 60 min [31]. Thus, any transcriptional alteration responsible for the acquired tolerance must occur within this early period after CO exposure. Therefore, 40 min of treatment with CORM-A1 was the chosen period for studying gene expression profiling. A total of 162 transcripts were found to be differentially expressed, being 100 of these genes upregulated and 62 downregulated by more than 1-fold in the CORM-A1 treated cultures, with a false discovery rate (FDR) < 0.05 (Supplementary Data Table S2).

Gene ontology analysis using GOMiner showed the "primary metabolic processes" as one of the most represented categories regulated upon exposure of astrocytes to CO (Fig. 2a), representing 10% of all altered genes (data not shown). This category includes, for example, the metabolic processes of carbohydrates, cellular amino acids, lipids and proteins, and the tricarboxylic acid cycle. These reactions guarantee the cellular basic needs, especially the energy status. This result is in accordance with the evidence for a role of CO in the modulation of mitochondrial function [6, 11, 27, 28]. Functional annotation also showed that genes acting on the control of gene expression and on the response to stimuli were the biological processes presenting higher amounts of
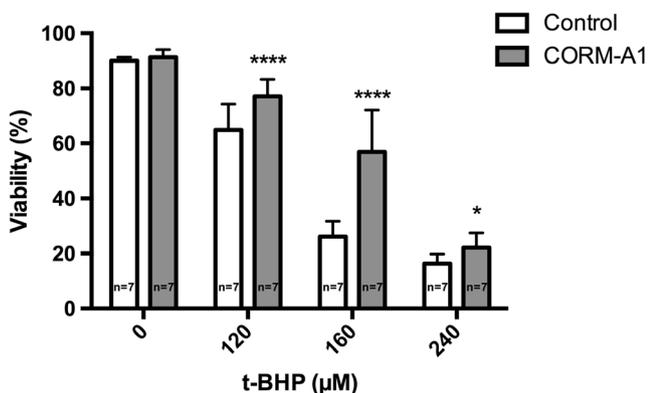

Fig. 1 CORM-A1 prevents astrocytic cell death. Primary cultures of cortical astrocytes were exposed to the pro-oxidant t-BHP. Astrocyte viability was assessed by PI internalization. Cortical astrocytes were stimulated with t-BHP (120 μM or 160 μM) for 20 h, prior to evaluation of cell viability. When the effect of CO was tested, the cells were pre-incubated with 12.5 μM CORM-A1 for 1 h before exposure to t-BHQ. The viability of cortical astrocytes was assessed by plasma membrane permeabilization by the uptake of PI. The results are the mean ± SEM of seven independent experiments, performed in different cell preparations. *$p < 0.1$, ****$p < 0.001$ compared to control with one-way ANOVA followed by Dunnett's post test

upregulated genes upon treatment of astrocytes with CO (Fig. 2a). This is not surprising since HO-1, the inducible endogenous enzyme producing CO, is a stress response gene, whose expression contributes to the cellular response against deleterious events, boosting cytoprotection, and tissue tolerance [35, 36]. Likewise, CO may trigger other cellular pathways which allow reacting against stressful stimuli, thus resulting in an overall upregulation of genes belonging to the categories of this ontology. Interestingly, the only biological process presenting higher levels of downregulated DEGs than upregulated DEGs was "cell differentiation" (Fig. 2a). In the last few years, evidence became available for effects of CO on differentiation of neuronal cells [7, 27], T cells [37], and cardiomyocytes [38]. Nevertheless, one reason for CO to promote differentiation might reside on its ability to modulate cell metabolism, cell death and redox responses, rather than triggering specific differentiation pathways.

When evaluating the molecular functions of the DEG regulated by CO in astrocytes, protein and ion binding are the major actions of the upregulated genes, representing 39% (Fig. 2c). On the other hand, downregulated DEGs mainly display functions related with catalytic activity, which represent a total of 26% (Fig. 2b). In addition to the functional annotation of the DEGs, we also analyzed whether there was any gene family represented by more than one gene. A total of 11 gene families were found, namely, Rho GTPase activating protein (Arhgap#, downregulated), Coiled-coil domain-containing protein (Ccdc#, mostly upregulated), family with sequence similarity (Fam#, downregulated), FBJ Murine Osteosarcoma Viral Oncogene Homolog (Fos, upregulated), interleukin receptors (Il#r, upregulated), protocadherins (Pcdh), protein tyrosine phosphatase (Ptp, downregulated), ribosomal RNA (Rn#s, downregulated), solute carrier family (Slc#a#, mostly downregulated), wingless-type MMTV integration site family (Wnt#), and Zinc finger proteins (Zfp#, upregulated). Altogether, these families represent 16.7% of the 162 DEGs.

In addition to the functional annotation of the DEGs, we used SABiosciences' proprietary database DECipherment of DNA Elements (DECODE, http://www.sabiosciences.com/chipqpcrsearch.php?app=TFBS) to identify transcription factors, upstream the identified DEGs, which are therefore likely to be candidate gene regulators in CO-triggered cytoprotection in astrocytes (Table 1). This analysis identified several targets of the transcriptional mediators of AP-1, Jun, HNF, and STAT. Thus, CO mainly modulates the expression of genes regulated by AP-1, Jun, HNF, and STAT transcription factors in cortical astrocytes.

In order to filter down the 162 DEGs to a workable number, we applied sequential filters to reduce down to 7 the number of DEGs used in additional validation steps (Fig. 3). The top 59 DEGs (33 upregulated and 26 downregulated) were shown to play relevant roles in the brain, both under physiological or
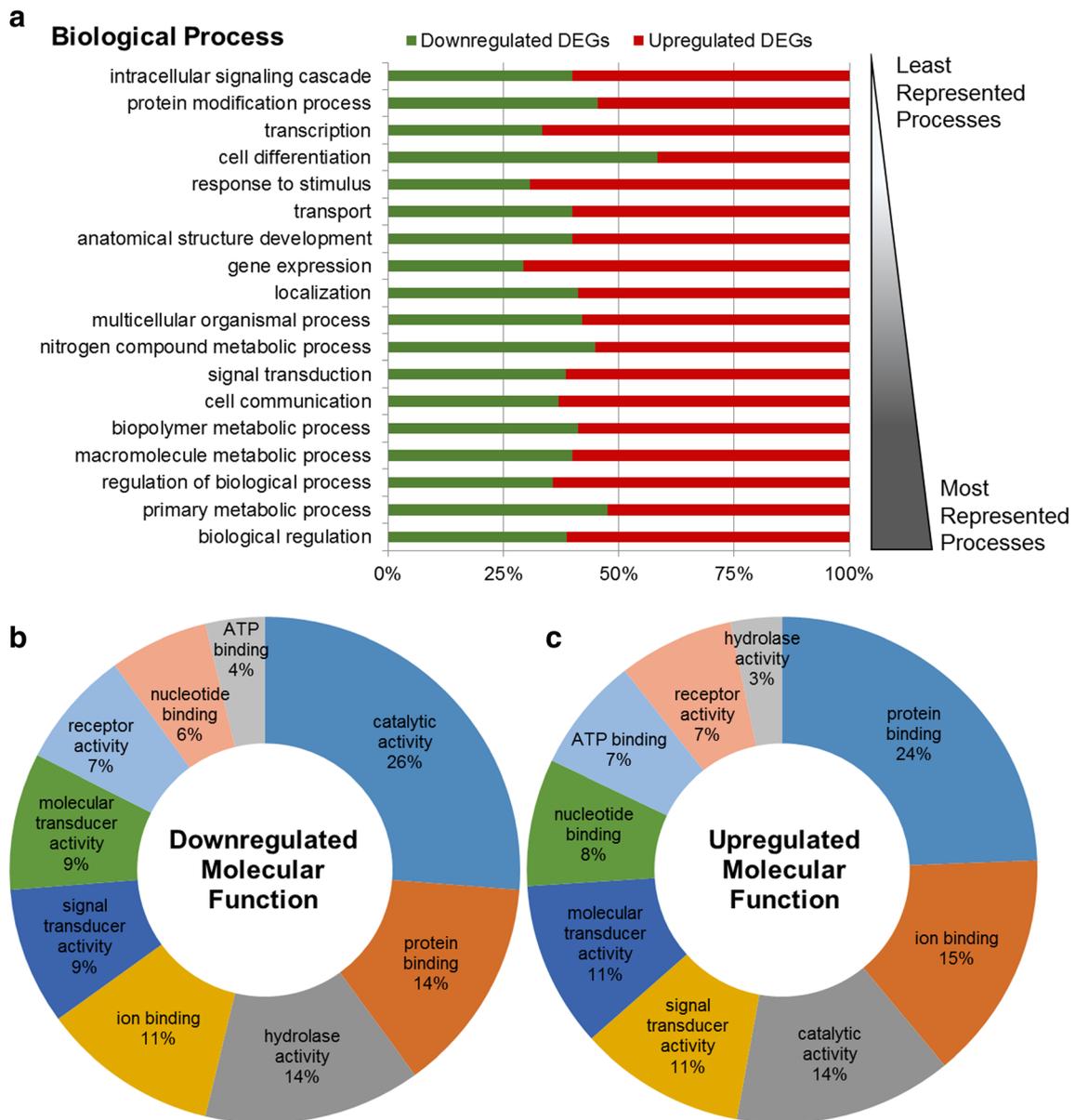
Fig. 2 Classification of DEG by function. **a** Biological processes represented among the differentially expressed genes (DEGs) detected following treatment of cortical astrocytes with CORM-A1. The percentage of up-regulated and down-regulated DEGs in each biological processes was determined using GoMiner. **b, c** Most represented molecular functions among CORM-A1-induced DEGs in cortical astrocytes. Cultured astrocytes were incubated with 12.5 μM CORM-A1 for 40 min. Molecular functions of upregulated (**b**) and downregulated (**c**) DEGs, as analyzed by GoMiner

pathological conditions, namely in ischemia, inflammation, neurogenesis, energy balance, and redox response. From this smaller group of DEGs, we further selected the ones common to at least two of the three algorithms applied in DEGs screening. This filtering step ensures a higher confidence on the candidate genes under analysis. The latter filter resulted in a group of 14 potential candidate DEGs (9 upregulated and 5 downregulated). Finally, a pool of 7 DEGs out of the previous 14 was selected based on their function and identified based on previously described effects of CO such as neuroprotection and calcium signaling [39]. In summary, we identified 162

DEGs in astrocytes treated with CO; metabolic and signaling pathways were found to be the most affected by CO treatment.

CO Induces FosB, Rgs10, and Scand1 Transcription in Cortical Astrocytes

From the 162 CO-induced DEGs, 7 genes were selected to be validated by qRT-PCR. As mentioned above, this subset of DEGs was chosen by two main criteria: (i) their expression was identified to be significantly altered by two of the three algorithms used and (ii) the candidate DEGs were relevant in

Table 1 Transcription factors regulating CO-induced DEG. The most represented transcription factors that regulate CORM-A1-induced DEGs in cortical astrocytes. Enriched transcription factors were identified by SABiosciences database (http://www.sabiosciences.com/chipqpcrsearch.php?app=TFBS)

	Transcription factors										
	AP	JUN	HNF	STAT	MYC	NFkB	PAX	GATA	PPAR	POU#F	ATF
Differentially expressed genes	Cish	Cyth1	Aass	Cish	Aspscr1	Dpp4	Ccdc85c	Aass	Dpp4	Aass	Dpp4
	Cyth1	Dab1	Ccdc85c	Hmgb1	Camta1	Hmgb1	Ndufb2	Hmgb1	Fap	Lars2	FosB
	Dab1	FosB	Dpp4	Il2ra	Dpp4	Il2ra	Pcsk1n	Map3k14	Gadd45a	Ndufb2	Lrrtm2
	Gadd45a	Gadd45a	Nkain4	Il2ra	Gadd45a	Lrrc23	Pde10a	Npr1	Srd5a1	Pik3cd	Ndufb2
	Il2ra	Il2ra	Rps6ka1	Lrrtm2	Gli2	Pik3cd	Pex12	Pixnd1	Wnt7a	Sic4a10	Pcsk1n
	Lrrc23	Lrrc23	Scand1	Ndufb2	Kdm4b	Rps6ka1	Zbtb20	Rarres2			
	Nkain4	Ndufb2	Srd5a1	Scand1	Wnt7a	Ugcg					
	Pex12	Nkain4	Stk36	Tnfsf13b							
	Tnfsf13b	Tnfsf13b	Wnt7a								

the context of this study (Fig. 3). Thus, changes in FosB (FBJ osteosarcoma oncogene B), Rgs10 (regulator of G-protein signaling 10), Scand1 (SCAN domain-containing 1), Rn18s (18S ribosomal RNA), Actg1 (actin, gamma, cytoplasmic 1), Pcdhb21 (protocadherin beta 21), and Panx1 (pannexin 1) mRNA levels were quantified in cultured cortical astrocytes incubated with CORM-A1 (12.5 μM) for 30 to 60 min. We confirmed the results obtained for three DEGs from the seven selected: FosB, Rgs10, and Scand1 (Fig. 4a–c). The Rn18s qRT-PCR data (Fig. 4d) showed a 2-fold increase in gene expression following incubation of astrocytes with CORM-A1, which contrasts with the results obtained in the RNASeq experiments (3.71-fold decrease). This discrepancy may be due to the fact that these two techniques identify
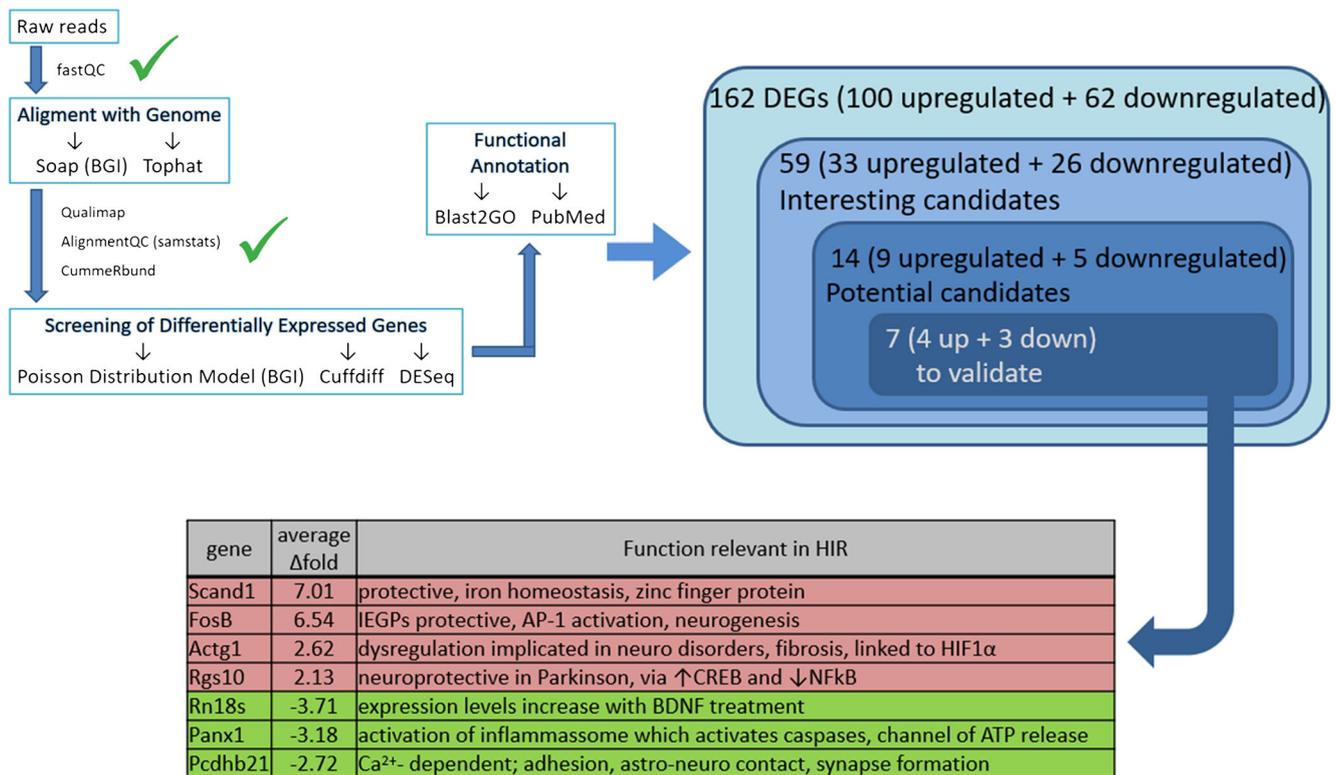

Fig. 3 RNASeq selection. Analysis and filtering steps applied to the RNASeq data for the effects of CO on gene expression in astrocytes. The upper right corner represents the different filters used to obtain the final 7 DEGs to validate: from the 162 DEGs, 59 candidates were interesting for being relevant in the brain; these 59 candidates were further filtered to 14 candidates due to their high potential as mediators of the response to CO. The table presents the seven DEGs selected for RT-PCR validation, their fold change and some of their relevant functions
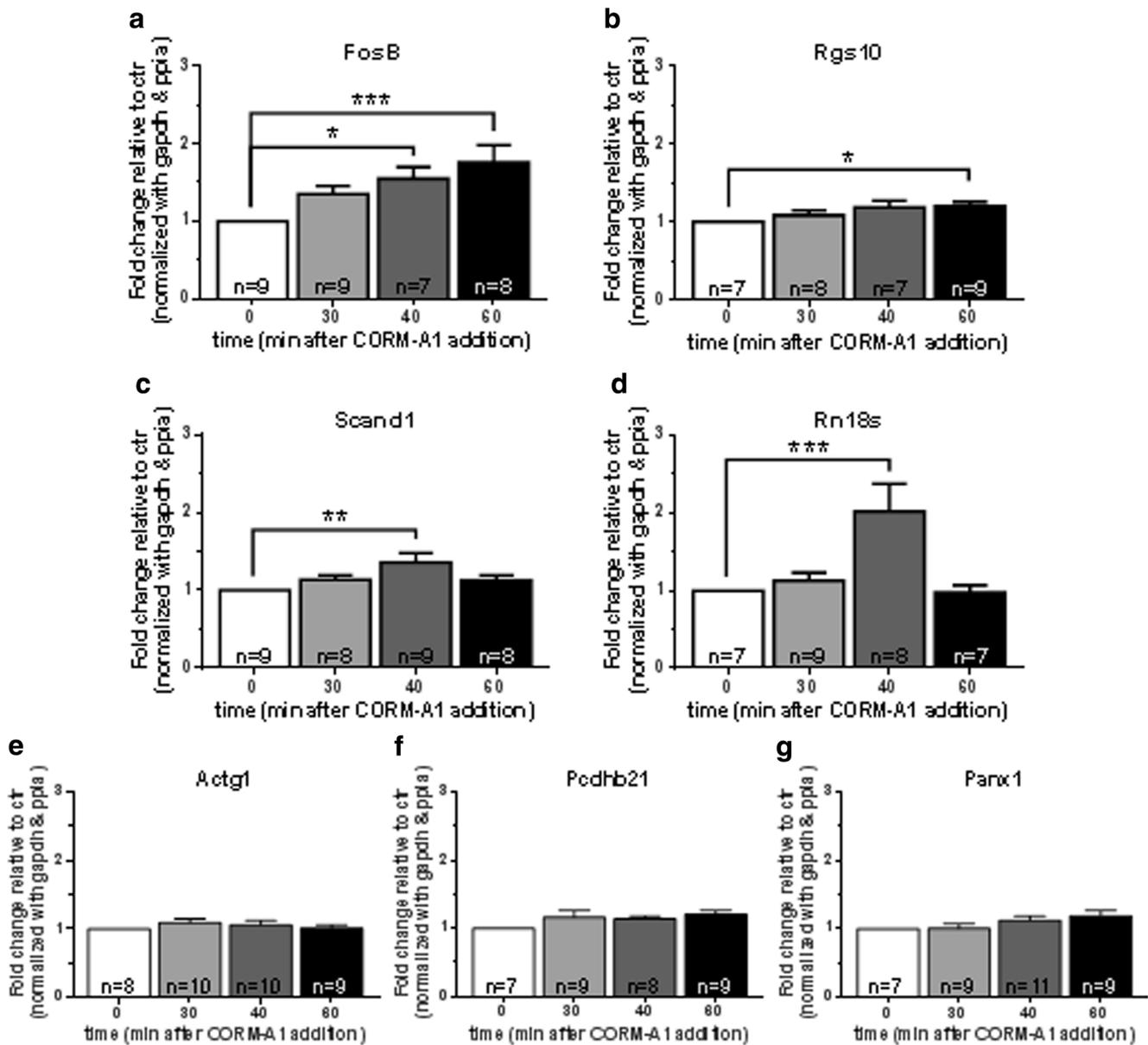
Fig. 4 Validation of CORM-A1 effect on gene expression by RT-Q-PCR. Effects of CORM-A1 on gene expression in cultured cortical astrocytes. Fold change in the expression of *FosB* (**a**), *Rgs10* (**b**), *Scand1* (**c**), *Rn18s* (**d**), *Actg1* (**e**), *Pcdhb21* (**f**), and *Panx1* (**g**) was analyzed by qPCR (see the "Material and Methods" section for further details). Cortical astrocytes were incubated with CORM-A (12.5 μM) for 30 to 60 min. The results are the mean ± SEM of at least nine independent experiments, performed in different cell preparations. *$p < 0.1$, **$p < 0.05$, and ***$p < 0.01$ as compared to the control with one-way ANOVA followed by Dunnett's post test

alterations in gene expression based on different assumptions and algorithms. The other three DEGs did not present a significant variation in expression when analyzed by qRT-PCR: Actg1, Pcdhb21, and Panx1 (Fig. 4e–g). Since FosB showed the strongest alteration in mRNA expression among the three genes validated, this gene was chosen for protein and functional validation. Interestingly, FosB is a component of AP-1, one of the most represented transcription factors identified based in the analysis of the CO-evoked changes in gene expression in astrocytes (Table 1).

CO Induces Cytoprotective AP-1 Products Expression

The activator protein-1 transcription factor (AP-1) is formed by FosB paired with Jun family members [40]. To better understand the consequences of FosB induction, and ultimately AP-1 activation, the regulation of several downstream targets was analyzed (Fig. 5). AP-1 induction mediates the cellular response to several stimuli, particularly the redox response, cell cycle, cell death control, and inflammation. Besides controlling a wide variety of biological processes, AP-1
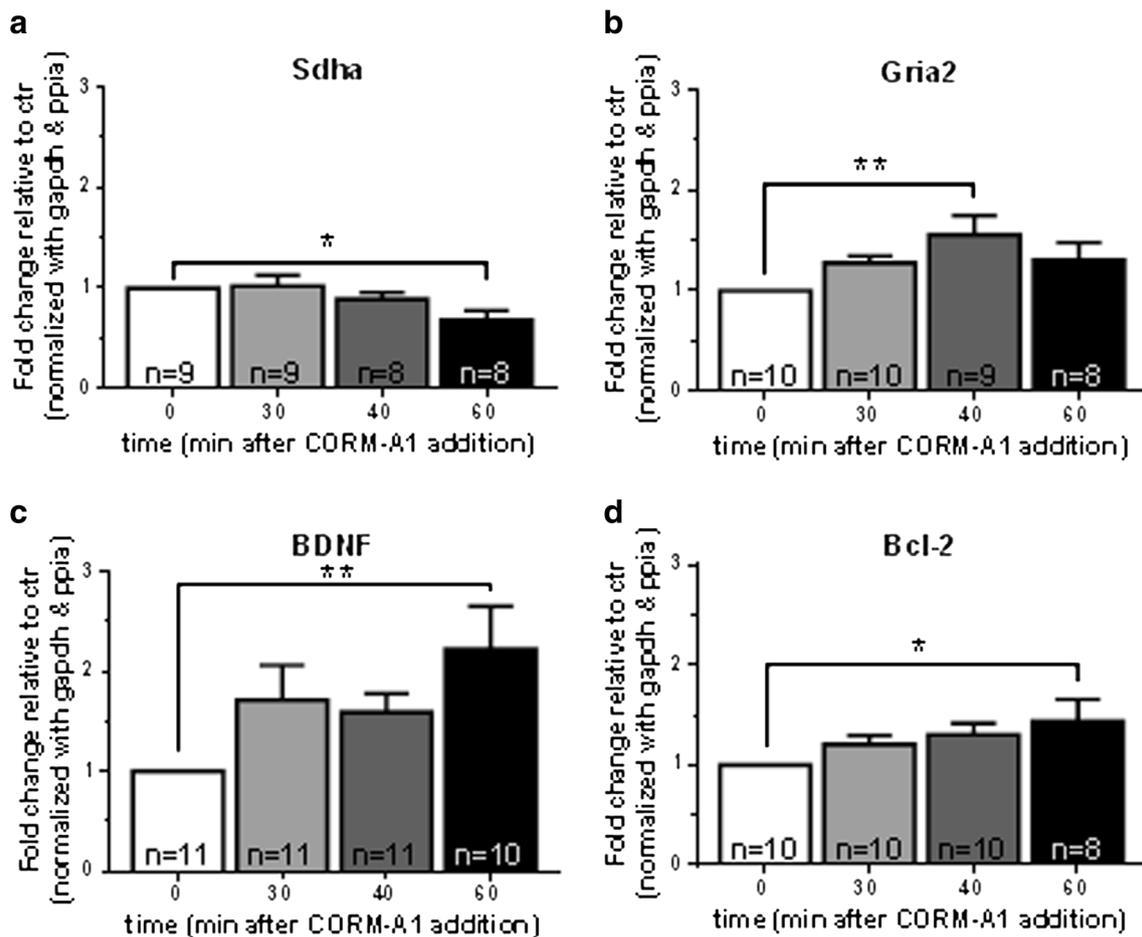
Fig. 5 Effects of CORM-A1 on the expression of AP-1 target genes in cultured cortical astrocytes. The cells were incubated with 12.5 μM CORM-A1 for the indicated periods of time. Fold change in the expression of AP-1 target genes (*Sdha*, *Bdnf*, *Bcl-2*, and *Gria2*) was analyzed by the $2^{-\Delta Ct}$ (see the "Material and Methods" section for further details). The results are the mean ± SEM of at least eight independent experiments, performed in different cell preparations. *$p < 0.1$ and **$p < 0.05$ as compared to the control with one-way ANOVA followed by Dunnett's post test

expression may induce bidirectional responses [41]: its negative or positive regulation of a specific pathway depends on the type of dimers formed within the cellular context [42, 43].

Alterations in the expression of several AP-1 target genes following stimulation of cortical astrocytes with CORM-A1 (12.5 μM for 30 to 60 min) were confirmed by qRT–PCR. These AP-1 target genes are the following: Gria2 (gene coding for glutamate ionotropic receptor AMPA type subunit 2) [44], BDNF [45] and Bcl-2 [46] (Fig. 5b–d, respectively). Importantly, the expression of two classical genes with a role in cell survival signaling was upregulated: Bdnf and Bcl-2 (Fig. 5c, d) [47, 48]. An increased membrane availability of GluA2-containing AMPAR was also proposed to provide protection against excitotoxic damage [49–51]. Since it was observed that Gria2 is upregulated after 40 min of incubation with CORM-A1, ultimately this event may also contribute to an increased tolerance to ischemia due to CO treatment.

Because mitochondria play a critical role in cell fate [52, 53] and are involved in CO-induced pathways [54, 55], a gene involved in mitochondrial function was also studied. Sdha is a gene coding for a major catalytic subunit of the complex II of the electron chain and its expression levels were quantified following CO treatment (Fig. 5a). As Sdha inhibition was described to be protective in an ischemia context [56–58], the observed downregulation in Sdha expression after 60 min of CO treatment may also contribute to the overall tendency for cell survival.

In conclusion, incubation of cortical astrocytes with CORM-A1 may activate multiple pathways, including the AP-1 transcription factor, which together may contribute to protect astrocytes against stress conditions.

CO Induces FosB Protein Expression and Promotes Astrocytic Survival by a Mechanism Dependent on P2X7 Receptor Activation

Validation of CO-induced FosB expression was performed by analyzing changes in protein expression following treatment of

astrocytes with CORM-A1 (12.5 μM). iCORM-A1 and CO gas were used as negative and positive controls, respectively, for the CO-induced effect on FosB expression (Supplementary Figure S2). The immunoblotting results showed a transient increase of FosB protein expression following 40 min of CO treatment; FosB protein levels returned to the baseline 20 min later and were maintained at basal levels for up to 5 h (Fig. 6). Thus, CO does promote Fos expression in a transient manner.

Recent studies showed that activation of the purinergic P2X7 receptor (P2X7R) results in a robust induction of FosB in monocytic and osteoblastic cells [59, 60]. Considering that (i) activation of P2X receptors is implicated in the role of CO in astrocyte-neuron paracrine neuroprotection [29] and (ii) P2X7R astrocytic expression was reported to be essential in ischemic preconditioning and cytoprotection [61], we investigated whether CO-induced FosB expression is mediated by P2X7R activation. Primary cultures of cortical astrocytes were treated with A-438079, a specific P2X7R inhibitor, for 10 min prior to CORM-A1 addition, and FosB protein levels were quantified after 40 min of incubation with CORM-A1 (Fig. 7a, b). The P2X7R inhibitor abrogated the effect of CORM-A1 on increasing FosB protein expression. These results suggest that CO promotes an autocrine effect, which could be mediated by the release of ATP from cortical astrocytes. Indeed, CO increases ATP production in astrocytes [6], which can be released to the extracellular environment [29].

In order to assess whether CORM-A1-induced cytoprotection is dependent on P2X7R activation, astrocytes pre-treated with CORM-A1, in the presence or absence of

P2X7R inhibitor A-438079, were challenged to death with the pro-oxidant agent *tert*-butylhydroperoxide (t-BHP). Inhibition of P2X7R abrogated the protective effects of CORM-A1 in astrocytes incubated with (t-BHP) (Fig. 7c), showing a role for P2X7R activity in the response to CO.

To further confirm that CO activates P2X7R, phosphorylation of Calmodulin was assessed in the presence of CORM-A1. In fact, activation of P2X7R increases intracellular calcium concentration, resulting in calcium/calmodulin-dependent protein kinase II (CaMKII) phosphorylation [62]. Protein expression of total and phosphorylated CaMKII was assessed following CORM-A1 treatment at 0, 1, 2, and 3 h (Fig. 8). CORM-A1 promoted CaMKII phosphorylation in a time-dependent manner. Thus, CaMKII activation is an indirect manner to corroborate the results showing CO-induced P2X7R activation.

CO-Induced Cytoprotection Is Independent on FosB Expression in Astrocytes

Astrocytes, followed by microglia, are the neural cells that present the highest levels of FosB expression [63]. This high expression of FosB in glia cells suggest an important function of this IEG, both under physiologic and pathologic conditions [64–67]. To determine whether FosB is essential in CO-induced cytoprotection, its expression was downregulated using a specific siRNA. To confirm the silencing of the gene, FosB expression was analyzed by Western blot at 12, 24, and 48 h after siRNA transfection (Supplementary Figure S3).
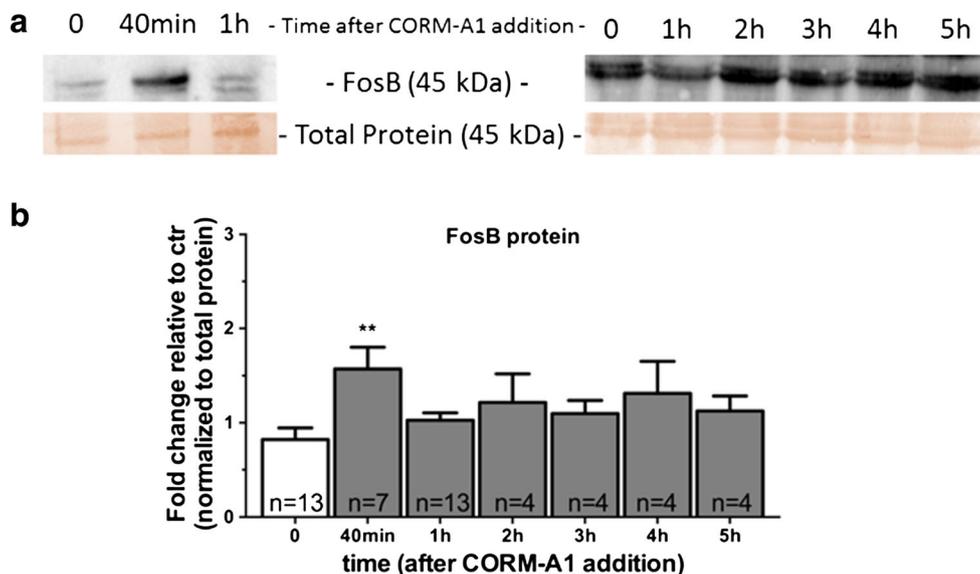

Fig. 6 Effect of CORM-A1 on the expression of the FosB protein in cultured cortical astrocytes. **a** Representative blots of immune detection of FosB and respective loading control with Rouge Ponceau. The first image corresponds to astrocytes treated with CORM-A1 after 0 min, 40 min, and 1 h (early effects) and the second image corresponds to astrocytes treated with CORM-A1 after 0 min, 1 h, 2 h, 3 h, 4 h, and

5 h (later effects). **b** Fold change in the expression of *FosB* was analyzed by western blot. The results are the mean ± SEM of at least four independent experiments, performed in different cell preparations and normalized to total protein. Total protein was evaluated by Rouge Ponceau staining. **p < 0.05 as compared to the control with one-way ANOVA followed by Dunnett's post test
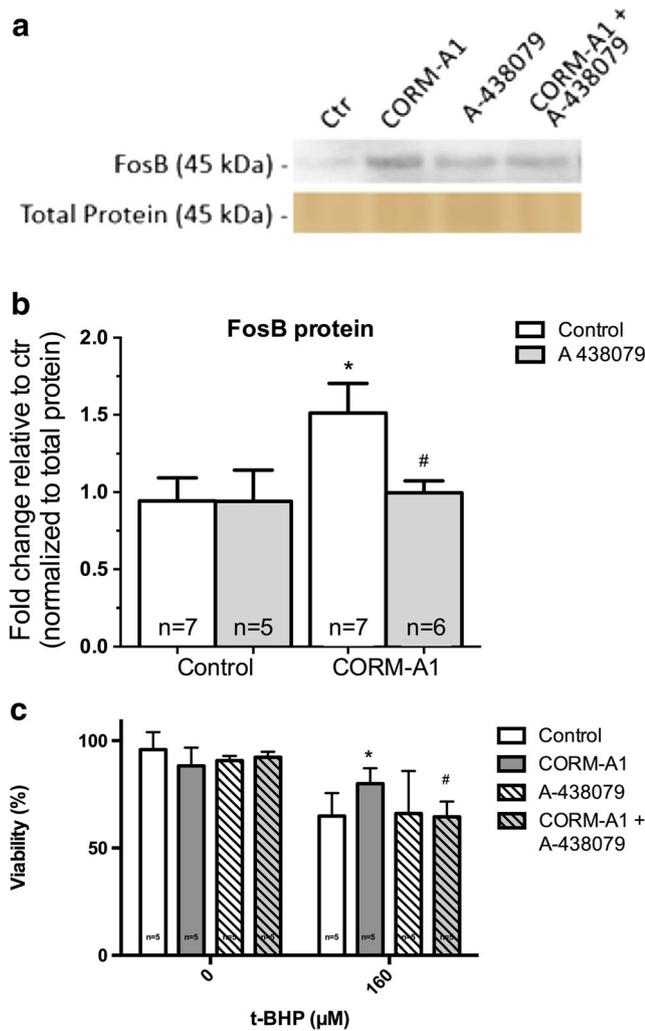
Fig. 7 Role of P2X7R in CORM-A1-induced expression of FosB and CORM-A1-induced cytoprotection in cultured cortical astrocytes. **a** Representative blot of immune detection of FosB and respective loading control with Rouge Ponceau. The lanes correspond respectively to astrocytes without treatment, or treated with CORM-A1 for 40 min, in the presence or in the absence of the P2X7R inhibitor (A-438079; 10 μM). **b** Fold change in the expression of *FosB* after 40 min of incubation with CORM-A1 (12.5 μM) was analyzed by western blot. The results are the mean ± SEM of at least five independent experiments, performed in different cell preparations and normalized to total protein. Total protein was evaluated by Rouge Ponceau staining. $*p < 0.05$ as compared to the control without CORM-A1 and $^{\#}p < 0.05$ as compared to the control without A-438079 with one-way ANOVA. **c** Astrocytic viability was assessed by PI following oxidative stress-induced cell death. The results are the mean ± SEM of five independent experiments. $*p < 0.01$ compared to control and $^{\#}p < 0.05$ compared to CORM-A1 without inhibitor with two-way ANOVA followed by Dunnett's post test

Since FosB downregulation was more efficient at 48 h, FosB silenced astrocytes were used within this time frame.

Astrocytic cell death induced by the pro-oxidant t-BHP (160 μM) was assessed by PI internalization, by measuring plasmatic membrane integrity. Astrocytic cultures that were pre-treated with CORM-A1 showed a significant decrease in
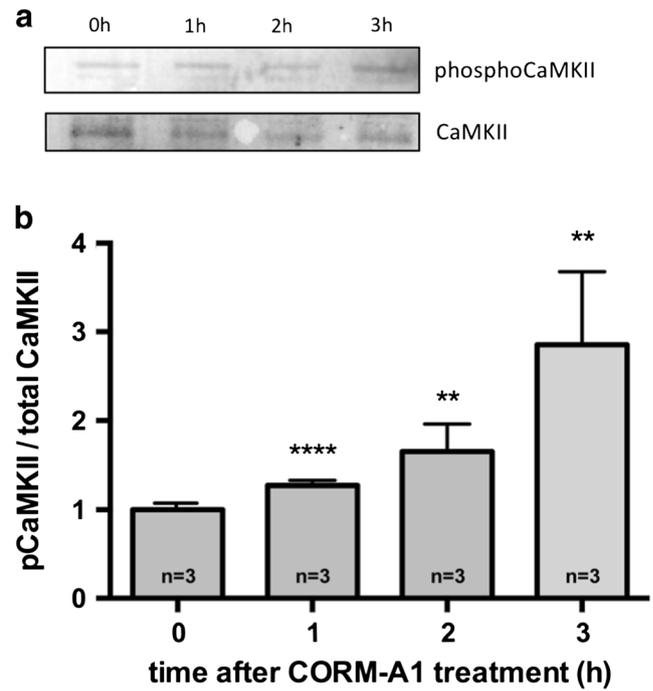

Fig. 8 CORM-A1 phosphorylates CaMKII. **a** Representative blot of immune detection of total CaMKII and phosphorylated CaMKII. Lanes correspond to astrocytes treated with CORM-A1 (12.5 μM) for 0, 1, 2, and 3 h. **b** Fold change in the ratio between phosphorylated and total CaMKII, the results are the mean ± SEM of three independent experiments, performed in different cell preparations. $**p < 0.01$ and $****p < 0.001$ compared to control (0 h) with unpaired Student's *t* test

cell death when exposed to 160 μM t-BHP, as expected (Fig. 9). Nevertheless, knocking down FosB did not affect the cytoprotective effect of CO, suggesting that despite being upregulated by CO, FosB is not essential for the protective effects of the gasotransmitter. Surprisingly, a significant
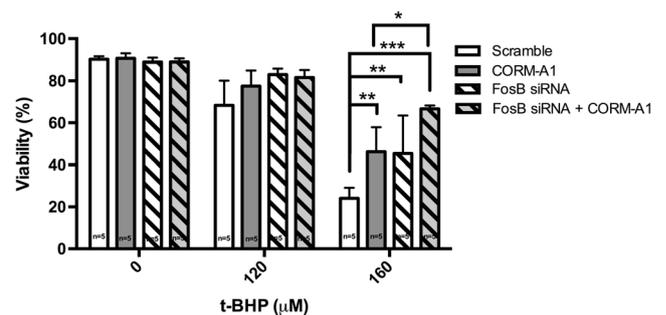

Fig. 9 Role of FosB in CORM-A1-induced cytoprotection of cortical astrocytes exposed to t-BHP. Astrocyte viability was assessed by PI internalization. Cortical astrocytes were stimulated with t-BHP (120 μM or 160 μM) for 20 h, before evaluation of cell viability. Where indicated, cells were pre-treated with an siRNA against FosB. The effect of CORM-A1 was tested by pre-incubating the cells with the CO-donor for 1 h before stimulation with t-BHP. The results are the mean ± SD of five independent experiments, performed in different cell preparations. $*p < 0.05$, $**p < 0.01$, and $***p < 0.001$ as compared to the respective scramble with two-way ANOVA with Tukey's multiple comparisons post test

cytoprotective effect was observed upon knocking down FosB expression (Fig. 9).

Discussion

In order to characterize the CO-induced alterations in gene expression, the whole transcriptome from cultured cortical astrocytes was sequenced using the RNASeq technique and DEGs were identified with Poisson Distribution Model, Cuffdiff and DESeq programs. Applying RNASeq in CO research brings novelty to the field since it allows the discovery of unmapped effectors of the gasotransmitter, for example transcripts resulting from alternative splicing or novel isoforms. Additionally, another advantage of RNASeq regarding microarrays is the fact that this technique is quantitative and allows the identification of transcripts with lower abundance. Furthermore, since we addressed this question at a fairly early time point following CO exposure the approach used is expected to identify initial players contributing to CO-induced cytoprotection. Pathway analysis and functional annotation were performed via GoMiner. Several genes were identified, opening future and novel potential lines of research in CO's Biology field. Following a careful DEG data analysis, an important candidate gene was pointed out: the FBJ murine osteosarcoma viral oncogene homolog B (FosB). Indeed, CO treatment did increase the expression of FosB gene at mRNA and protein levels in astrocytes, which were assessed by qRT-PCR and Western blot techniques, respectively.

The CO-induced upregulation of FosB protein expression in cultured astrocytes was found to be transient, reaching its maximal at 40 min and returning to basal levels after 1 h of treatment. As FosB is an immediate early gene, its expression occurs within a short time window, and presents a short half-life, upon a wide range of stimuli [42, 68, 69]. The FosB C-terminus contains two degron domains (amino acid sequences that regulate its own degradation rates), which are recognized as a signal for ubiquitination and proteasome-mediated degradation [70]. Herein, we report a very transient effect of CORM-A1 on the expression of the FosB protein. Upon CO treatment, the abundance of FosB protein decreased back to control levels at a faster rate than FosB transient induction by drugs of abuse [71]. This difference can be explained by several factors: (i) the majority of FosB studies in brain tissue were performed in neurons, and the machinery involved in the regulation of the protein half-life in astrocytes may be distinct; (ii) differences in the nature of the stimulus; and (iii) CO may modulate the major pathways involved in FosB degradation. Indeed, CO decreases iNOS protein levels in hepatocytes by inducing autophagy and the ubiquitin-proteasome system [72].

In the present study, CORM-A1 was found to induce the expression of FosB by a mechanism dependent on the activation of P2X7 receptors. P2X7R activation has been shown to trigger FosB expression in different models [60, 73]. Furthermore, P2X7Rs have been implicated in cell death signaling, both in astrocytes [74, 75] and other cells [76, 77]. Likewise, we showed that inhibition of P2X7R abrogated the protective effects of CORM-A1 in astrocytes exposed to t-BHP. In addition, astrocytes treated with CORM-A1 presented higher levels of phosphorylated CaMKII, a P2X7R downstream kinase. In fact, the presence and function of P2X7R in cortical astrocytes has been largely documented [73, 78–80], and these receptors have a protective role in brain ischemia [61, 81].

Finally, the protective effect of CORM-A1 in cortical astrocytes subjected to oxidative stress conditions was found to be independent of FosB expression. These data open new possibilities concerning the mechanisms underlying the protective effects of CO: (i) CO-induced protection in astrocytes may depend on the combined activity of different pathways and, therefore, inhibition of one of the mechanisms involved does not change the effect of the gasotransmitter on cell survival; (ii) astrocytes may upregulate other components of AP-1 to compensate for the lack of FosB; (iii) a prolonged blockage of AP-1 activation is beneficial and further protection may be achieved when CORM-A1 is added by activation of anti-apoptotic pathways (e.g., Bdnf, Bcl-2); (iv) upon downregulation of FosB, its truncated isoform may be expressed in a compensatory form to contribute to cytoprotection; and (v) CO-induced FosB expression may not be relevant in the protection of astrocytes by CO. The role of FosB and its isoforms has been studied most comprehensively in the context of drug addiction, but a building body of evidence also points to an important beneficial role for FosB in several pathologies, namely seizures [82], ischemia [83–85], hypoglycemia [86], nurturing defect [87, 88], and Parkinson's disease [89]. However, further studies are required to understand the role FosB role and its mechanisms of action in these pathologies.

The AP-1 transcription factor is mainly composed of either heterodimers of c-Jun/c-Fos or homodimers of c-Jun. It has been reported that ERK signaling pathway leads to activation of c-Fos, while JNK leads to c-Jun activation. The ERK pathway induces cell proliferation and differentiation, whereas the JNK pathway mediates inhibition of proliferation or cell death [42, 44, 59, 90]. The results obtained in the RNASeq experiments suggest that Jun family members are not regulated by CO treatment, since no members of this family were identified in the DEGs list (Supplementary Data Table S2), at least after 40 min of incubation with CORM-A1. Nevertheless, the cytoprotective effects of CO/HO-1 have been partially linked to AP-1 modulation via c-Fos-Jun

[90–93]. Thus, it remains to be determined whether CO modulates FosB containing AP-1 and its potential role in CO-induced cytoprotection. Likewise, in the TGF-β1-dependent apoptosis, only the JunD and FosB components of AP-1 are significantly induced [94]. The same might occur in CO-dependent AP-1 induction. In the present study, we found that CORM-A1 enhances the expression of FosB in cortical astrocytes. Other AP-1 components, such as the c-Jun, are known to be expressed after CO treatment, as in the case of astrocytes exposed to CORM-2 [95]. Additional studies are required to identify FosB binding partners in this context. Besides c-Jun, JunB is a probable candidate as it presents a similar induction profile to FosB in astrocytes after glutamate treatment [96].

The observed CO-induced increase in the expression of Bdnf is in accordance with previous results [31, 97]. Similarly, the Bcl-2 induction following CO administration was also previously described [6, 7, 13, 25, 98]. These pieces of evidence support the data showing CO as an important gas in the control of cell survival, since both Bdnf and Bcl-2 are anti-apoptotic players and can contribute to the protective actions of CO. Moreover, inhibition of TrkB receptors was shown to abrogate neuroprotection prompted by CO in astrocytes [29], further corroborating the key role of Bdnf in the protective effects of the gasotransmitter.

In conclusion, the current study indicates that CORM-A1 reduces the apoptotic death of cortical astrocytes subjected to oxidative stress conditions through activation of P2X7R and by a mechanism independent of FosB. Additional studies are required to identify the pathways acting downstream of P2X7R activation in the protection of astrocytes by CO. Furthermore, complementary in vivo studies should be performed to confirm the role of P2X7R in CO-induced cytoprotection in astrocytes and how astrocytes can promote neuroprotection. The new DEG identified in astrocytes treated with CO open new opportunities for studying pathways mediating the cytoprotection role of the gasotransmitter.

Author's Contributions SRO performed experimental procedures and carried out the analysis and interpretation of data. CFP performed experimental procedures. HLAV and CBD participated in the discussion of data and critically reviewed the manuscript. SRO, HLAV, and CBD participated in the conception and design of the study, as well as in the analysis and interpretation of data. All authors read and approved the final manuscript.

References

1. Wegiel B, Hanto DW, Otterbein LE (2013) The social network of carbon monoxide in medicine. Trends Mol Med 19:3–11. https://doi.org/10.1016/j.molmed.2012.10.001

2. Queiroga CSF, Vercelli A, Vieira HLA (2015) Carbon monoxide and the CNS: challenges and achievements. Br J Pharmacol 172:1533–1545. https://doi.org/10.1111/bph.12729

3. Schallner N, Romão CC, Biermann J et al (2013) Carbon Monoxide Abrogates Ischemic Insult to Neuronal Cells via the Soluble Guanylate Cyclase-cGMP Pathway. PLoS One 8. https://doi.org/10.1371/journal.pone.0060672

4. Vieira HLA, Queiroga CSF, Alves PM (2008) Pre-conditioning induced by carbon monoxide provides neuronal protection against apoptosis. J Neurochem 107:375–384. https://doi.org/10.1111/j.1471-4159.2008.05610.x

5. Queiroga CSF, Almeida AS, Martel C et al (2010) Glutathionylation of adenine nucleotide translocase induced by carbon monoxide prevents mitochondrial membrane permeabilization and apoptosis. J Biol Chem 285:17077–17088. https://doi.org/10.1074/jbc.M109.065052

6. Almeida AS, Queiroga CSF, Sousa MFQ et al (2012) Carbon monoxide modulates apoptosis by reinforcing oxidative metabolism in astrocytes: Role of Bcl-2. J Biol Chem 287:10761–10770. https://doi.org/10.1074/jbc.M111.306738

7. Almeida AS, Soares NLNL, Vieira M et al (2016) Carbon monoxide releasing molecule-A1 (CORM-A1) improves neurogenesis: increase of neuronal differentiation yield by preventing cell death. PLoS One 11:e0154781. https://doi.org/10.1371/journal.pone.0154781

8. Bani-Hani MG, Greenstein D, Mann BE et al (2006) Modulation of thrombin-induced neuroinflammation in BV-2 microglia by carbon monoxide-releasing molecule 3. J Pharmacol Exp Ther 318:1315–1322. https://doi.org/10.1124/jpet.106.104729

9. Foresti R, Bains SK, Pitchumony TS et al (2013) Small molecule activators of the Nrf2-HO-1 antioxidant axis modulate heme metabolism and inflammation in BV2 microglia cells. Pharmacol Res 76:132–148. https://doi.org/10.1016/j.phrs.2013.07.010

10. Ulbrich F, Goebel U, Böhringer D et al (2016) Carbon monoxide treatment reduces microglial activation in the ischemic rat retina. Graefes Arch Clin Exp Ophthalmol 254:1967–1976. https://doi.org/10.1007/s00417-016-3435-6

11. Wilson JLJL, Bouillaud F, Almeida AS et al (2017) Carbon monoxide reverses the metabolic adaptation of microglia cells to an inflammatory stimulus. Free Radic Biol Med 104:311–323. https://doi.org/10.1016/j.freeradbiomed.2017.01.022

12. Wang B, Cao W, Biswal S, Doré S (2011) Carbon monoxide-activated Nrf2 pathway leads to protection against permanent focal cerebral ischemia. Stroke 42:2605–2610. https://doi.org/10.1161/STROKEAHA.110.607101

13. Queiroga CSF, Tomasi S, Widerøe M et al (2012) Preconditioning triggered by carbon monoxide (co) provides neuronal protection following perinatal hypoxia-ischemia. PLoS One 7. https://doi.org/10.1371/journal.pone.0042632

14. Yabluchanskiy A, Sawle P, Homer-Vanniasinkam S et al (2012) CORM-3, a carbon monoxide-releasing molecule, alters the inflammatory response and reduces brain damage in a rat model of hemorrhagic stroke. Crit Care Med 40:544–552. https://doi.org/10.1097/CCM.0b013e31822f0d64

15. Chora ÂA, Fontoura P, Cunha A et al (2007) Heme oxygenase–1 and carbon monoxide suppress autoimmune neuroinflammation. J Clin Invest 117:438–447. https://doi.org/10.1172/JCI28844

16. Fagone P, Mangano K, Quattrocchi C et al (2011) Prevention of clinical and histological signs of proteolipid protein (PLP)-induced experimental allergic encephalomyelitis (EAE) in mice by the water-soluble carbon monoxide-releasing molecule (CORM)-A1. Clin Exp Immunol 163:368–374. https://doi.org/10.1111/j.1365-2249.2010.04303.x

17. Motterlini R, Clark JE, Foresti R et al (2002) Carbon monoxide-releasing molecules: characterization of biochemical and vascular activities. Circ Res 90:e17–e24. https://doi.org/10.1161/hh0202.104530

18. Romão CC, Blättler WA, Seixas JD, Bernardes GJL (2012) Developing drug molecules for therapy with carbon monoxide. Chem Soc Rev 41:3571. https://doi.org/10.1039/c2cs15317c

19. Motterlini R, Sawle P, Hammad J et al (2005) CORM-A1: a new pharmacologically active carbon monoxide-releasing molecule. FASEB J 19:284–286. https://doi.org/10.1096/fj.04-2169fje

20. Allaman I, Be M, Magistretti PJ (2011) Astrocyte – neuron metabolic relationships: for better and for worse. Trends Neurosci 34. https://doi.org/10.1016/j.tins.2010.12.001

21. Cahoy JD, Emery B, Kaushal A et al (2008) A transcriptome database for astrocytes, neurons, and oligodendrocytes: a new resource for understanding brain development and function. J Neurosci 28:264–278. https://doi.org/10.1523/JNEUROSCI.4178-07.2008

22. Dulak J, Józkowicz A (2003) Carbon monoxide — a "new" gaseous modulator of gene expression. Acta Biochim Pol 50:31–47

23. Ryter SW, Choi AMK (2016) Targeting heme oxygenase-1 and carbon monoxide for therapeutic modulation of inflammation. Transl Res 167:7–34

24. Ryter SW, Morse D, Choi AMK (2004) Carbon monoxide: to boldly go where NO has gone before. Sci STKE 27:3145–3165. https://doi.org/10.1002/cpe.3463

25. Schallner N, Fuchs M, Schwer CI et al (2012) Postconditioning with inhaled carbon monoxide counteracts apoptosis and neuroinflammation in the ischemic rat retina. PLoS One 7. https://doi.org/10.1371/journal.pone.0046479

26. Pellerin L, Magistretti PJ (2012) Sweet sixteen for ANLS. J Cereb Blood Flow Metab 32:1152–1166. https://doi.org/10.1038/jcbfm.2011.149

27. Almeida AS, Sonnewald U, Alves PM, Vieira HLA (2016) Carbon monoxide improves neuronal differentiation and yield by increasing the functioning and number of mitochondria. J Neurochem 138:423–435. https://doi.org/10.1111/jnc.13653

28. Wegiel B, Gallo D, Csizmadia E et al (2013) Carbon monoxide expedites metabolic exhaustion to inhibit tumor growth. Cancer Res 73:7009–7021. https://doi.org/10.1158/0008-5472.CAN-13-1075

29. Queiroga CSF, Alves RMA, Conde SV et al (2016) Paracrine effect of carbon monoxide: astrocytes promote neuroprotection via purinergic signaling. J Cell Sci 129:jcs.187260. https://doi.org/10.1242/jcs.187260

30. Hertz L, Juurlink BHJ, Hertz E, Fosmark H, Schousboe A (1989) Preparation of primary cultures of mouse (rat) astrocytes. In: Shahar A, De Vellis J, Vernadakis A, Haber B (eds) A dissection and tissue culture manual for the nervous system, Alan R. Liss, New York, pp 105–108

31. Oliveira SR, Vieira HLA, Duarte CB (2015) Effect of carbon monoxide on gene expression in cerebrocortical astrocytes: Validation

32. of reference genes for quantitative real-time PCR. Nitric Oxide Biol Chem 49:80–89. https://doi.org/10.1016/j.niox.2015.07.003

32. Livak KJ, Schmittgen TD (2001) Analysis of relative gene expression data using real-time quantitative PCR and the 2^(-2ΔΔCt) Method. Methods 25:402–408. https://doi.org/10.1006/meth.2001.1262

33. Ficker C, Rozmer K, Kató E et al (2014) Astrocyte-neuron interaction in the substantia gelatinosa of the spinal cord dorsal horn via P2X7 receptor-mediated release of glutamate and reactive oxygen species. Glia 62:1671–1686. https://doi.org/10.1002/glia.22707

34. Leichsenring A, Riedel T, Qin Y et al (2013) Anoxic depolarization of hippocampal astrocytes: possible modulation by P2X7 receptors. Neurochem Int 62:15–22. https://doi.org/10.1016/j.neuint.2012.11.002

35. Motterlini R, Foresti R (2014) Heme oxygenase-1 as a target for drug discovery. Antioxid Redox Signal 20:1810–1826. https://doi.org/10.1089/ars.2013.5658

36. Agarwal A, Bolisetty S (2013) Adaptive responses to tissue injury: role of heme oxygenase-1. Trans Am Clin Climatol Assoc 124:111–122

37. Nikolic I, Vujicic M, Stojanovic I et al (2014) Carbon monoxide-releasing molecule-A1 inhibits Th1/Th17 and stimulates Th2 differentiation in vitro. Scand J Immunol 80:95–100. https://doi.org/10.1111/sji.12189

38. Suliman HB, Zobi F, Piantadosi CA (2016) Heme oxygenase-1/carbon monoxide system and embryonic stem cell differentiation and maturation into cardiomyocytes. Antioxid Redox Signal 24:345–360. https://doi.org/10.1089/ars.2015.6342

39. Oliveira SR, Queiroga CSF, Vieira HLA et al (2016) Mitochondria and carbon monoxide: cytoprotection and control of cell metabolism - a role for Ca 2+ ? J Physiol 00:6–8. https://doi.org/10.1113/JP270955

40. Chinenov Y, Kerppola TK (2001) Close encounters of many kinds: Fos-Jun interactions that mediate transcription regulatory specificity. Oncogene 20:2438–2452. https://doi.org/10.1038/sj.onc.1204385

41. Shaulian E, Karin M (2002) AP-1 as a regulator of cell life and death. Nat Cell Biol 4:E131–E136. https://doi.org/10.1038/ncb0502-e131

42. Hess J, Angel P, Schorpp-Kistner M (2004) AP-1 subunits: quarrel and harmony among siblings. J Cell Sci 117:5965–5973. https://doi.org/10.1242/jcs.01589

43. Vesely PW, Staber PB, Hoefler G, Kenner L (2009) Translational regulation mechanisms of AP-1 proteins. Mutat Res Rev Mutat Res 682:7–12. https://doi.org/10.1016/j.mrrev.2009.01.001

44. Wang Q, Li W, Liu XS et al (2011) ERK-associated changes of AP-1 proteins during fear extinction. Mol Cell Neurosci 47:137–144. https://doi.org/10.1016/j.molcel.2007.05.041.A

45. Pruunsild P, Orav E, Esvald E (2013) AP-1 transcription factors mediate BDNF-Positive Feedback Loop in Cortical Neurons. J Neurosci 36:1290–1305. https://doi.org/10.1523/JNEUROSCI.3360-15.2016

46. Hu S, Zhang Y, Zhang M et al (2015) Aloperine protects mice against ischemia-reperfusion (IR)-induced renal injury by regulating PI3K/AKT/mTOR signaling and AP-1 Activity. Mol Med 21:912–923. https://doi.org/10.2119/molmed.2015.00056

47. Melo CV, Okumoto S, Gomes JR et al (2013) Spatiotemporal resolution of BDNF neuroprotection against glutamate excitotoxicity in cultured hippocampal neurons. Neuroscience 237:66–86. https://doi.org/10.1016/j.neuroscience.2013.01.054

48. Jonas EA, Porter GA, Alavian KN (2014) Bcl-xL in neuroprotection and plasticity. Front Physiol 5:355. https://doi.org/10.3389/fphys.2014.00355

49. Van Damme P, Bogaert E, Dewil M et al (2007) Astrocytes regulate GluR2 expression in motor neurons and their vulnerability to

excitotoxicity. Proc Natl Acad Sci U S A 104:14825–14830. https://doi.org/10.1073/pnas.0705046104

50. Xu Y, Xue H, Zhao P (et al, 2016) Isoflurane postconditioning induces concentration- and timing-dependent neuroprotection partly mediated by the GluR2 AMPA receptor in neonatal rats after brain hypoxia–ischemia. J Anesth:1–10. https://doi.org/10.1007/s00540-015-2132-7

51. Wang H, Luo M, Li C, Wang G (2011) Propofol post-conditioning induced long-term neuroprotection and reduced internalization of AMPAR GluR2 subunit in a rat model of focal cerebral ischemia/reperfusion. J Neurochem 119:210–219. https://doi.org/10.1111/j.1471-4159.2011.07400.x

52. Bhola PD, Letai A (2016) Mitochondria—Judges and executioners of cell death sentences. Mol Cell 61:695–704. https://doi.org/10.1016/j.molcel.2016.02.019

53. Yonutas HM, Vekaria HJ, Sullivan PG (2016) Mitochondrial specific therapeutic targets following brain injury. Brain Res 1640:77–93. https://doi.org/10.1016/j.brainres.2016.02.007

54. Almeida AS, Figueiredo-Pereira C, Vieira HLA (2015) Carbon monoxide and mitochondria - modulation of cell metabolism, redox response and cell death. Front Physiol 6:1–6. https://doi.org/10.3389/fphys.2015.00033

55. Queiroga CSF, Almeida AS, Vieira HLA (2012, 2012) Carbon monoxide targeting mitochondria. Biochem Res Int:1–9. https://doi.org/10.1155/2012/749845

56. Dröse S (2013) Differential effects of complex II on mitochondrial ROS production and their relation to cardioprotective pre- and postconditioning. Biochim Biophys Acta Bioenerg 1827:578–587. https://doi.org/10.1016/j.bbabio.2013.01.004

57. Grimm S (2013) Respiratory chain complex II as general sensor for apoptosis. Biochim Biophys Acta 1827:565–572. https://doi.org/10.1016/j.bbabio.2012.09.009

58. Hoshi A, Nakahara T, Ogata M, Yamamoto T (2005) The critical threshold of 3-nitropropionic acid-induced ischemic tolerance in the rat. Brain Res 1050:33–39. https://doi.org/10.1016/j.brainres.2005.05.028

59. Gavala ML, Hill LM, Lenertz LY et al (2010) Activation of the transcription factor FosB/activating protein-1 (AP-1) is a prominent downstream signal of the extracellular nucleotide receptor P2RX7 in monocytic and osteoblastic cells. J Biol Chem 285:34288–34298. https://doi.org/10.1074/jbc.M110.142091

60. Lenertz LY, Gavala ML, Zhu Y, Bertics PJ (2011) Transcriptional control mechanisms associated with the nucleotide receptor P2X7, a critical regulator of immunologic, osteogenic and neurologic functions. Immunol Res 50:22–38. https://doi.org/10.1007/s12026-011-8203-4.Transcriptional

61. Hirayama Y, Ikeda-Matsuo Y, Notomi S et al (2015) Astrocyte-mediated ischemic tolerance. J Neurosci 35:3794–3805. https://doi.org/10.1523/JNEUROSCI.4218-14.2015

62. León D, Hervás C, Miras-Portugal MT (2006) P2Y 1 and P2X 7 receptors induce calcium/calmodulin-dependent protein kinase II phosphorylation in cerebellar granule neurons. Eur J Neurosci 23:2999–3013. https://doi.org/10.1111/j.1460-9568.2006.04832.x

63. Zhang Y, Chen K, Sloan SA et al (2014) An RNA-sequencing transcriptome and splicing database of glia, neurons, and vascular cells of the cerebral cortex. J Neurosci 34:11929–11947. https://doi.org/10.1523/JNEUROSCI.1860-14.2014

64. Kuroda KO, Ornthanalai VG, Kato T, Murphy NP (2010) FosB null mutant mice show enhanced methamphetamine neurotoxicity: potential involvement of FosB in intracellular feedback signaling and astroglial function. Neuropsychopharmacology 35:641–655. https://doi.org/10.1038/npp.2009.169

65. Peng L, Li B, Du T et al (2010) Astrocytic transactivation by alpha2A-adrenergic and 5-HT2B serotonergic signaling. Neurochem Int 57:421–431. https://doi.org/10.1016/j.neuint.2010.04.018

66. Li B, Du T, Li H et al (2008) Signalling pathways for transactivation by dexmedetomidine of epidermal growth factor receptors in astrocytes and its paracrine effect on neurons. Br J Pharmacol 154:191–203. https://doi.org/10.1038/bjp.2008.58

67. Yutsudo N, Kamada T, Kajitani K et al (2013) fosB-Null Mice Display Impaired Adult Hippocampal Neurogenesis and Spontaneous Epilepsy with Depressive Behavior. Neuropsychopharmacology 38:895–906. https://doi.org/10.1038/npp.2012.260

68. Zerial M, Toschi L, Ryseck RP et al (1989) The product of a novel growth factor activated gene, fos B, interacts with JUN proteins enhancing their DNA binding activity. EMBO J 8:805–813

69. Alibhai IN, Green TA, Potashkin JA, Nestler EJ (2007) Regulation of fosB and ∆fosB mRNA expression: in vivo and in vitro studies. Brain Res 1143:22–33. https://doi.org/10.1016/j.brainres.2007.01.069

70. Carle TL, Ohnishi YN, Ohnishi YH et al (2007) Proteasome-dependent and -independent mechanisms for FosB destabilization: identification of FosB degron domains and implications for ∆FosB stability. Eur J Neurosci 25:3009–3019. https://doi.org/10.1111/j.1460-9568.2007.05575.x

71. Nestler EJ (2012) Transcriptional mechanisms of drug addiction. Clin Psychopharmacol Neurosci 10:136–143. https://doi.org/10.9758/cpn.2012.10.3.136

72. Kim HS, Loughran PA, Billiar TR (2008) Carbon monoxide decreases the level of iNOS protein and active dimer in IL-1beta-stimulated hepatocytes. Nitric Oxide 18:256–265. https://doi.org/10.1016/j.niox.2008.02.002

73. Wickert LE, Blanchette JB, Waldschmidt NV et al (2013) The C-terminus of human nucleotide receptor P2X7 is critical for receptor oligomerization and N-linked glycosylation. PLoS One 8. https://doi.org/10.1371/journal.pone.0063789

74. Salas E, Carrasquero LMG, Olivos-Oré LA et al (2013) Purinergic P2X7 receptors mediate cell death in mouse cerebellar astrocytes in culture. J Pharmacol Exp Ther 347:802–815. https://doi.org/10.1124/jpet.113.209452

75. Gandelman M, Peluffo H, Beckman JS et al (2010) Extracellular ATP and the P2X7 receptor in astrocyte-mediated motor neuron death: implications for amyotrophic lateral sclerosis. J Neuroinflammation 7:33. https://doi.org/10.1186/1742-2094-7-33

76. Chu K, Yin B, Wang J et al (2012) Inhibition of P2X7 receptor ameliorates transient global cerebral ischemia/reperfusion injury via modulating inflammatory responses in the rat hippocampus. J Neuroinflammation 9:69

77. Arbeloa J, Pérez-Samartín A, Gottlieb M, Matute C (2012) P2X7 receptor blockade prevents ATP excitotoxicity in neurons and reduces brain damage after ischemia. Neurobiol Dis 45:954–961. https://doi.org/10.1016/j.nbd.2011.12.014

78. Alloisio S, Aiello R, Ferroni S, Nobile M (2006) Potentiation of native and recombinant P2X7-mediated calcium signaling by arachidonic acid in cultured cortical astrocytes and human embryonic kidney 293 cells. Mol Pharmacol 69:1975–1983. https://doi.org/10.1124/mol.105.020164

79. Nobile M, Monaldi I, Alloisio S et al (2003) ATP-induced, sustained calcium signalling in cultured rat cortical astrocytes: evidence for a non-capacitative, P2X7-like-mediated calcium entry. FEBS Lett 538:71–76

80. Nagasawa K, Escartin C, Swanson RA (2009) Astrocyte cultures exhibit P2X7 receptor channel opening in the absence of exogenous ligands. Glia 57:622–633. https://doi.org/10.1002/glia.20791

81. Franke H, Illes P (2014) Nucleotide signaling in astrogliosis. Neurosci Lett 565:14–22. https://doi.org/10.1016/j.neulet.2013.09.056

82. Giordano C, Vinet J, Curia G, Biagini G (2015) Repeated 6-Hz corneal stimulation progressively increases FosB/δFosB levels in the lateral amygdala and induces seizure generalization to the

Hippocampus. PLoS One 10:1–21. https://doi.org/10.1371/journal.pone.0141221

83. Kurushima H, Ohno M, Miura T et al (2005) Selective induction of DeltaFosB in the brain after transient forebrain ischemia accompanied by an increased expression of galectin-1, and the implication of DeltaFosB and galectin-1 in neuroprotection and neurogenesis. Cell Death Differ 12:1078–1096. https://doi.org/10.1038/sj.cdd.4401648

84. Alfonso-Jaume MA, Bergman MR, Mahimkar R et al (2006) Cardiac ischemia-reperfusion injury induces matrix metalloproteinase-2 expression through the AP-1 components FosB and JunB. Am J Physiol Heart Circ Physiol 291:H1838–H1846. https://doi.org/10.1152/ajpheart.00026.2006

85. Butler TL, Pennypacker KR (2004) Temporal and regional expression of Fos-related proteins in response to ischemic injury. Brain Res Bull 63:65–73. https://doi.org/10.1016/j.brainresbull.2003.12.005

86. Al-Noori S, Sanders NM, Taborsky GJ et al (2008) Recurrent hypoglycemia alters hypothalamic expression of the regulatory proteins FosB and synaptophysin. Am J Phys Regul Integr Comp Phys 295:R1446–R1454. https://doi.org/10.1152/ajpregu.90511.2008

87. Brown JR, Ye H, Bronson RT et al (1996) A defect in nurturing in mice lacking the immediate early gene fosB. Cell 86:297–309. https://doi.org/10.1016/S0092-8674(00)80101-4

88. Kuroda KO, Meaney MJ, Uetani N, Kato T (2008) Neurobehavioral basis of the impaired nurturing in mice lacking the immediate early gene FosB. Brain Res 1211:57–71. https://doi.org/10.1016/j.brainres.2008.02.100

89. Pavón N, Martín AB, Mendialdua A, Moratalla R (2006) ERK phosphorylation and FosB expression are associated with L-DOPA-induced dyskinesia in hemiparkinsonian mice. Biol Psychiatry 59:64–74. https://doi.org/10.1016/j.biopsych.2005.05.044

90. Morse D, Pischke SE, Zhou Z et al (2003) Suppression of inflammatory cytokine production by carbon monoxide involves the JNK pathway and AP-1. J Biol Chem 278:36993–36998. https://doi.org/10.1074/jbc.M302942200

91. Choi BM, Pae HO, Kim YM, Chung HT (2003) Nitric oxide-mediated cytoprotection of hepatocytes from glucose deprivation-induced cytotoxicity: Involvement of heme oxygenase-1. Hepatology 37:810–823. https://doi.org/10.1053/jhep.2003.50114

92. Serizawa F, Patterson E, Potter RF et al (2015) Pretreatment of human cerebrovascular endothelial cells with CO-releasing molecule-3 interferes with JNK/AP-1 signaling and suppresses LPS-induced proadhesive phenotype. Microcirculation 22:28–36. https://doi.org/10.1111/micc.12161

93. Cheng P-Y, Lee Y-M, Shih N-L et al (2006) Heme oxygenase-1 contributes to the cytoprotection of alpha-lipoic acid via activation of p44/42 mitogen-activated protein kinase in vascular smooth muscle cells. Free Radic Biol Med 40:1313–1322. https://doi.org/10.1016/j.freeradbiomed.2005.11.024

94. Yamamura Y, Hua X, Bergelson S, Lodish HF (2000) Critical role of Smads and AP-1 complex in transforming growth factor–dependent apoptosis. J Biol Chem 275:36295–36302. https://doi.org/10.1074/jbc.M006023200

95. Chi P-L, Lin C-C, Chen Y-W et al (2014) CO Induces Nrf2-dependent heme oxygenase-1 transcription by cooperating with Sp1 and c-Jun in rat brain astrocytes. Mol Neurobiol. https://doi.org/10.1007/s12035-014-8869-4

96. Condorelli DF, Dell'Albani P, Amico C et al (1993) Induction of primary response genes by excitatory amino acid receptor agonists in primary astroglial cultures. J Neurochem 60:877–885. https://doi.org/10.1111/j.1471-4159.1993.tb03232.x

97. Hung S-YS, Liou H-CH, Fu W-MW (2010) The mechanism of heme oxygenase-1 action involved in the enhancement of neurotrophic factor expression. Neuropharmacology 58:321–329. https://doi.org/10.1016/j.neuropharm.2009.11.003

98. Sener A, Tran KC, Deng JP et al (2013) Carbon monoxide releasing molecules inhibit cell death resulting from renal transplantation related stress. J Urol 190:772–778. https://doi.org/10.1016/j.juro.2012.12.020